WOODHEAD PUBLISHING SERIES IN CIVIL AND STRUCTURAL ENGINEERING

# DIAGNOSIS OF HERITAGE BUILDINGS BY NON-DESTRUCTIVE TECHNIQUES

Edited by
BLANCA TEJEDOR HERRÁN
AND DAVID BIENVENIDO-HUERTAS

ELSEVIER

Woodhead Publishing Series in Civil and Structural Engineering

# Diagnosis of Heritage Buildings by Non-Destructive Techniques

*Edited by*


*Blanca Tejedor Herrán*

**Dept. of Project and Construction Engineering Polytechnic University of Catalonia Barcelona Spain**

*David Bienvenido-Huertas*

**Dept. of Building Construction University of Granada Granada Spain**



ELSEVIER

WP WOODHEAD PUBLISHING

An imprint of Elsevier

Woodhead Publishing is an imprint of Elsevier
50 Hampshire Street, 5th Floor, Cambridge, MA 02139, United States
125 London Wall, London EC2Y 5AS, United Kingdom



**Notices**

Knowledge and best practice in this field are constantly changing. As new research and experience broaden our understanding, changes in research methods, professional practices, or medical treatment may become necessary.

Practitioners and researchers must always rely on their own experience and knowledge in evaluating and using any information, methods, compounds, or experiments described herein. In using such information or methods they should be mindful of their own safety and the safety of others, including parties for whom they have a professional responsibility.

To the fullest extent of the law, neither the Publisher nor the authors, contributors, or editors, assume any liability for any injury and/or damage to persons or property as a matter of products liability, negligence or otherwise, or from any use or operation of any methods, products, instructions, or ideas contained in the material herein.

ISBN: 978-0-443-16001-1 (print)
ISBN: 978-0-443-16002-8 (online)

For information on all Woodhead Publishing publications
visit our website at https://www.elsevier.com/books-and-journals

*Publisher:* Matthew Deans
*Acquisitions Editor:* Chiara Giglio
*Editorial Project Manager:* Emily Thomson
*Production Project Manager:* Erragounta Saibabu Rao
*Cover Designer:* Mark Rogers

Typeset by MPS Limited, Chennai, India

# Contents

# 3 Evaluation of the envelope airtightness by means of combined infrared thermography and pressurization tests in heritage buildings: A case study

*Irene Poza-Casado, Diego Tamayo-Alonso, Miguel Ángel Padilla-Marcos, and Alberto Meiss*
GIR Arquitectura & Energía, Dpto. Construcciones Arquitectónicas, Ingeniería del Terreno y Mecánica de los Medios Continuos y Teoría de Estructuras, Universidad de Valladolid, Valladolid, Spain

## 3.1 Introduction

### *3.1.1 Background*

Nowadays focus has been put on the reduction of the energy use of buildings. It is estimated that around 35% of the EU's buildings are over 50 years old and almost 75% of the building stock is energy-inefficient (Filippidou & Navarro, 2019). Hence, improving the energy performance not only of new buildings but also of the existing built stock is crucial to reach the EU's objectives (Directive 2018/844 amending Directive 2010/31/EU on the energy performance of buildings and Directive 2012/27/EU on energy efficiency, 18/844 Amending Directive 2010/31/EU on the Energy Performance of Buildings and Directive 2012/27/EU on Energy Efficiency, 2018). Strong long-term renovation strategies must be encouraged fostering deep energy retrofitting of existing buildings.

Therefore establishing solutions for the renovation of national building stocks and promoting their transformation into nearly zero-energy buildings seems necessary. The problem of energy loss caused by conduction through the building envelope has been significantly reduced by the development of advanced insulating materials, but it is frequently forgotten that the presence of air infiltration has a significant impact on the overall energy performance of buildings. Previous research estimated that 10%−30% of the heating demand is caused by air infiltration, which is mostly determined by the permeability of the building (Domínguez-Amarillo et al., 2019; Huang et al., 1999; Jokisalo et al., 2009; Jones et al., 2015; Kalamees, 2007; Meiss & Feijó-Muñoz, 2015; Simson et al., 2020; Zheng et al., 2020).

**Diagnosis of Heritage Buildings by Non-Destructive Techniques. DOI:** https://doi.org/10.1016/B978-0-443-16001-1.00003-6

Consequently, actions toward better energy efficiency will necessarily involve the improvement of the thermal performance of the exterior envelope including airtight solutions. Because leakages are hidden in walls and other cavities, it is difficult to increase the airtightness of existing buildings. Instead, leakage paths must be individually identified and sealed (Bohac et al., 2016), so special attention needs to be paid to the diagnosis stage.

In this context, historic buildings play a key role. Age in buildings hardly affects the presence of envelope leakages, but historic building techniques could not avoid them (Lerma et al., 2014). Nowadays technology allows for achieving almost perfect airtight envelopes by using special tapes and new building systems, which are effective for airtight joints between materials and mechanical parts and giving continuity to the built surfaces.

To assess historic buildings, non-destructive techniques (NDTs) need to be implemented. In the field of airtightness, several methods have been developed over the years (Charlesworth, 1988; Kronvall, 1980; McWilliams, 2003; Priestner & Steel, 1991; Zheng et al., 2020). Fan pressurization tests prevail due to their simplicity, time requirements, availability of commercial equipment, and mitigation of weather conditions by the pressure differential (Ashrae, 2021). Thus this NDT is considered reasonably accurate and reproducible (Sherman & Chan, 2004).

Pressurization tests provide quantitative information on the airtightness of a building, but this method does not address leakage location. Thus several methods have been reported in the literature to qualitatively assess leakages: smoke detection, anemometers, the soap bubble method, hand inspection, or helium-filled balloons (Pickering et al., 1987), but IR thermography (IRT), often combined with depressurization, seems to be the most widespread method (Kronvall, 1980). IRT technology is applied in old and new buildings to identify leakages in the building without affecting the finishing work (Lucchi, 2018).

The aim of this study consists of the development of a non-destructive methodology to evaluate the airtightness performance of the envelope and its application in a historic building. IRT was used while depressurizing the volume to locate the leakages along the envelope of the conditioned space. Knowing that the space is a residential retrofitted unit in a historical building, the evaluation of leakages can improve the global performance of the envelope to establish a strategy for energy retrofitting. This kind of building has been normally refurbished covering those existing historical structures, walls, floors, or roofs, which promotes indirect air leakage through unidentified air chambers in the building.

## 3.2 Materials and methods

### *3.2.1 Case study*

#### *3.2.1.1 History and context of the building*

The NDT methodology developed within this research was applied to a room of a historic building of Universidad de Valladolid (Spain), that is, the residence hall


**Figure 3.1 Palacio Santa Cruz.** View from Cardenal Mendoza Street.
*Source*: From Fundación Joaquín Díaz.

"Colegio Mayor Santa Cruz" (Fig. 3.1). This building was founded in 1483 and finished in 1491 as a protohumanist work whose purpose was to provide greater access to culturally inclined individuals accessing the university. The sponsor of this great institution was Don Pedro González de Mendoza, Cardinal Mendoza, whose purpose was to build a symbolic building for the institution. Today, this building is known as "Palacio Santa Cruz" and is the headquarter of the Rector's Office of Universidad de Valladolid (Ordax, 2005).

Later on, as a consequence of the time limit rule for the residents, the so-called Hospedería del Colegio Mayor Santa Cruz, a guesthouse dependent on the residence hall, was created. It seems that this category of "guest" residents was generalized at the end of the 16th century. In the guesthouse, although they were not proper residents, former residents continued to enjoy almost all the privileges—except the right to vote. Outsiders could also stay when they purchased a letter of brotherhood.

Historic sources make reference to the establishment of the guesthouse in the 16th century, in 1588. In addition, the need to expand its capacity made the residence hall buy several annex buildings between 1641 and 1649 (Fernández et al., 2010). This explains why when a guesthouse is built in the second half of the 17th century, it is referred to as a "new guesthouse" and the remains of an "old guesthouse" are mentioned in Fig. 3.2.

In 1675, Master Francisco de la Torre was commissioned to build a new guesthouse, whose common facilities and cells were organized around a cloister with four arches. This building has two floors and a square layout, and it was smaller in size than the residence hall. The exterior walls are made of a stone plinth and a

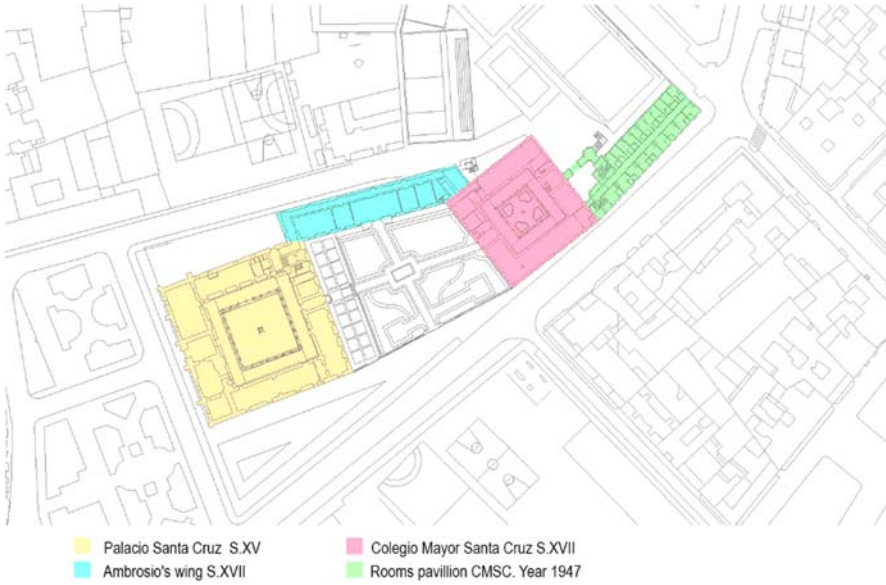


**Figure 3.2 Santa Cruz complex.** Historical evolution.

combination of masonry and brick, according to 17th-century preferences Fig. 3.3. The masonry is quite correct, with stones of great size, while the brickwork is done with a relatively thick tendril in which cracks are marked achieving a play of light and shade.

At the end of the 18th century, after many years of improper practices in the residence halls, guesthouses were eliminated, and the privileges of the residents definitively disappeared.

During the 19th and early 20th centuries, the Santa Cruz complex had different uses, such as the Episcopal Palace, the residence of General Wellington after the liberation of Valladolid from the French occupation, the prison, the School of Arts and Crafts, the Art Museum, Archaeological Museum, and headquarter of the Real Academy of the Purísima Concepción. Later on, in 1935, it became the Rector's Office of the University of Valladolid and the Archaeological Museum until 1968. Since 1929, the building has recovered its use as a residence hall (Ordax, 2005).

So many changes in its use led to continuous renovations over time, which were hardly ever documented. Only the renovations made by the end of the 20th century as a residence hall have been registered: a glass closure was installed in the first-floor corridor around the courtyard, and rooms with bathrooms and the director's house, which later became facilities for the students, were designed.

Currently, the guesthouse has six rooms with bathrooms, which are rented for short stays to university visitors. The building also comprises several facilities for the students who stay in the adjacent building, such as a study room, video library, dining room, living room, and auditorium.

**Figure 3.3 Guesthouse (current Santa Cruz Residence Hall).** Main facade.

### *3.2.1.2 Building characterization*

The building under study, "Hospedería del Colegio Mayor Santa Cruz," is located parallel to Cardenal Mendoza Street in the city center of Valladolid, near other historic buildings of the University. Its main facade faces southwest and can be accessed from the garden located between the guesthouse and Palacio Santa Cruz. The square-shaped building, 34 m on each side, stands free on all sides except for two corners, where it connects to the San Ambrosio wing and the rooms pavilion of the residence hall, as shown in Fig. 3.4.

The building is configured with a double concentric gallery with respect to the central courtyard. The exterior gallery is supported on 110 cm load-bearing walls made of brick and masonry, and the inner gallery used as a corridor is supported on the intermediate load-bearing wall and the arches on stone columns of the courtyard. Between these supports, wooden beams are placed, and on top of them, a wooden platform. Internal partitions are made of simple-hollow brick with plaster on both sides. In the bathrooms of the rooms, a marble floor is installed on this platform, as well as the walls' finishing. The rooms have a false ceiling with perimeter molding. The bathrooms also have a false ceiling, but in this case with an open perimeter groove. The windows are relatively recent, made of wood with double glazing with a chamber.

A suite room on the southeast facade, facing Cardenal Mendoza Street, was chosen as the area to be studied, according to the floor plan in Figs. 3.5−3.7. The name of the room honors a former resident, Juan de Marquina. Tests were carried out considering the whole suite but also excluding the volume of the bathroom.

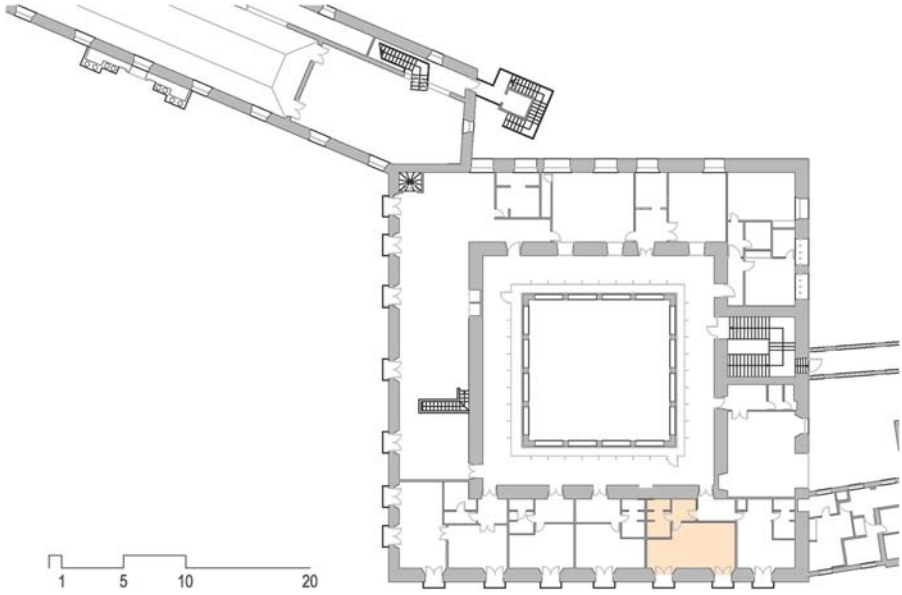


**Figure 3.4 Guesthouse.** First floor.

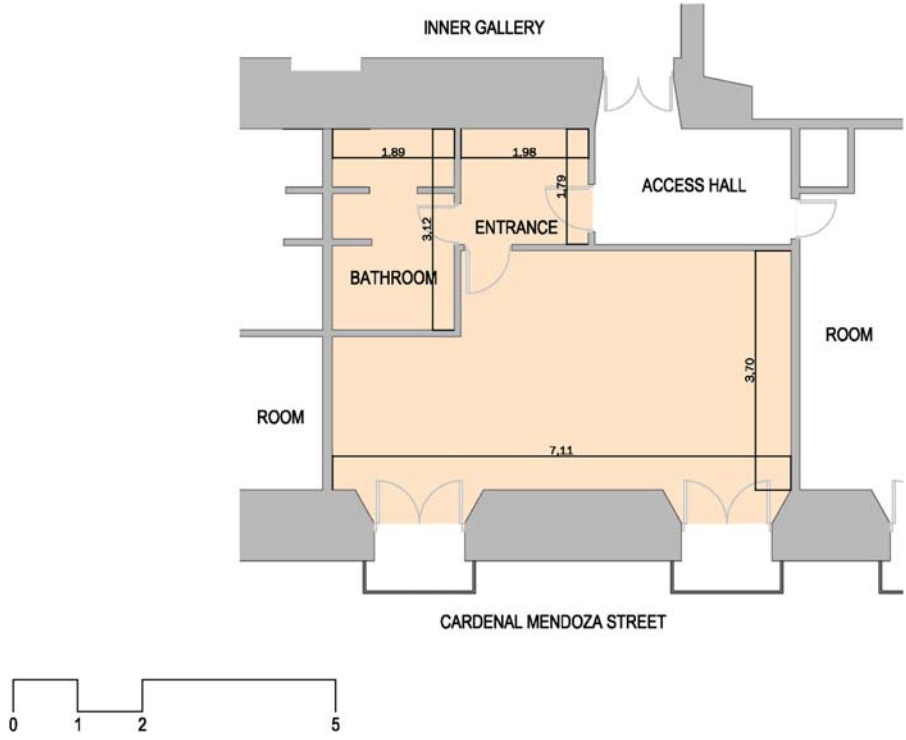


**Figure 3.5 Room of the guesthouse under study.** Testing area floor plan (dimensions in meters).

**Figure 3.6 Room of the guesthouse under study.** Elevation.

**Figure 3.7 Room of the guesthouse under study.** Interior layout.

The room is adjacent to two other rooms on the same floor, the exterior wall, and the nonconditioned corridor and access hall. Below, there are conditioned common facilities, whereas there is a crawl space above the room. This is a ventilated space, and it is partially insulated.

Table 3.1 shows the main dimensions of the room.

The room presents hardly any pathology. Only some cracks in the false ceiling were found, probably due to some movement of the building, after an intervention (Fig. 3.8).

The building's conditioning system, installed in the second half of the 20th century, consists of a diesel boiler, currently replaced by a gas boiler, and water radiators in the rooms. Regarding ventilation, there is only mechanical exhaust ventilation in the bathroom commanded by the bathroom light (Fig. 3.9). Fresh air enters the room through leakages in the envelope as a consequence of the depressurization caused by the exhaust.

### 3.2.2 Pressurization of the building envelope

The air permeability of the room envelope was measured by means of the fan pressurization method, also known as the blower door test, which has become the most widely method used to evaluate the airtightness of a building (Priestner & Steel, 1991). The equipment used was Minneapolis Blower Door Model 4. The test was performed according to ISO 9972,72 (2015). This test is meant to assess the airtightness of a whole building or a part of it, in this case, a room of the guesthouse. Therefore the room is treated as a single-zone building by opening interior doors in the adjacent rooms. In this sense, it is important to highlight that the envelope includes the boundary with the outdoor air but also with other conditioned rooms and unconditioned spaces, and this test does not provide information regarding the location of the leaks. Guarded-zone airtightness tests were not performed.

For the test, a fan temporarily replaces the main door of the space to be measured and generates a pressure difference between the inside and the outside of the room (Fig. 3.10). Depending on the position of the fan, the depressurization or pressurization of the room forces the entrance/exhaust of the outdoor/indoor air, respectively. In this way, the airtightness of the envelope is measured.

High wind speeds and indoor/outdoor temperature difference compromise the accuracy of the results. However, under favorable conditions, the generated pressure difference overcomes weather impact on the measurement.

The assessed room was prepared according to Method 2 described in ISO 9972. That is the measurement of the building envelope, with all intentional openings sealed. In this way, the bathroom exhaust was sealed, and the windows were closed.

Automated tests were carried out and monitored by the software provided by the blower door manufacturer (TECTITE Express). Before inducing any pressure by means of the fan, and also at the end of the test, the zero-flow pressure difference is evaluated over a period of 30 seconds to verify that the test has been performed according to the standard. Then, two sets of measurements, both pressurization and depressurization, are induced taking measurements of the airflow rate over a range of pressure differences between $\pm 16$ and $\pm 70$ Pa in increments of 6 Pa. These measurements determine the leakage function (log-log plot), which establishes a relationship between the airflow rate and the pressure difference (Ashrae, 2021) through the so-called power law:

$$Q_{pr} = c_L \cdot (\Delta p_r)^n$$

**Table 3.1** Main dimensions of the room under study.

| Room | Floor area | Height | Volume | Outdoor envelope area | Heated envelope area | Unconditioned envelope area | Total envelope area | Windows |
|---|---|---|---|---|---|---|---|---|
| Units | ($m^2$) | (m) | ($m^3$) | ($m^2$) | ($m^2$) | ($m^2$) | ($m^2$) | (m) |
| Whole room | 34.54 | 2.98 | 102.77 | 24.82 | 61.19 | 57.67 | 143.68 | 2 (1.4 × 2.4) |
| Room excluding the bathroom | 28.75 | 2.98 | 85.68 | 134.56 | 28.75 | 20.56 | 134.56 | 2 (1.4 × 2.4) |

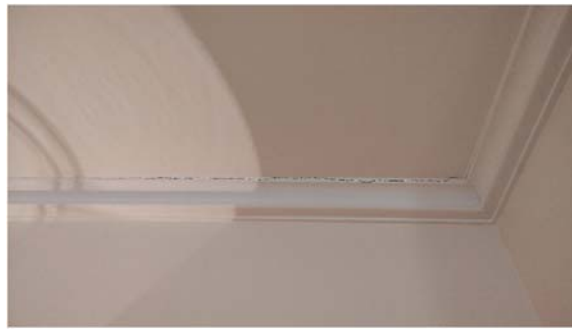

**Figure 3.8 Room of the guesthouse under study.** False ceiling pathology.

**Figure 3.9 Room of the guesthouse under study.** Bathroom extraction.

where $Q_{pr}$is the airflow rate of the opening at a reference pressure difference $\left[m^3/h\right]$; $C_L$ is the air leakage coefficient $\left[m^3/(hPa^n)\right]$; $\Delta p_r$ is the reference pressure difference $[Pa]$; $n$ is the airflow exponent $[-]$.

An ordinary least square regression was used for the calculation of the airflow characteristics (ISO 9972,72, 2015). The coefficient $n$ value must be in the range 0.5 and 1, and it provides information concerning the relative size of the leaks. Values near 0.5 are related to large leakages and short paths, whereas $n$ values close to 1 are usually found in airtight envelopes due to a steady laminar flow through small leakages (Allen, 1985).

The correct calibration of the equipment was ensured to maintain accuracy specifications of 1% of sampling, or 0.15 Pa to reduce uncertainties. The overall uncertainty in the parameters obtained was considered to remain below 10% under the calm conditions reported (ISO 9972,72, 2015).

Results are referred at a reference pressure of 50 Pa and normalized by both the inner volume ($V$) and envelope area ($A_E$), obtaining the air change rate ($n_{50}$) and the specific air leakage rate ($q_{50}$), as shown in the following equations:

$$n_{50} = Q_{50}/V$$


**Figure 3.10 Airtightness test layout.** Blower door system.

where $n_{50}$ is the air change rate at 50 Pa$\left[\mathrm{h}^{-1}\right]$; $Q_{50}$ is the air leakage rate at 50 Pa$\left[\mathrm{m}^3/\mathrm{h}\right]$; and $V$ is the internal volume $\left[\mathrm{m}^3\right]$.

$$q_{50} = Q_{50}/A_E$$

where $q_{50}$is the specific leakage rate per the building envelope area at 50 Pa$\left[\mathrm{m}^3/\mathrm{hm}^2\right]$; $Q_{50}$ is the air leakage rate at 50 Pa$\left[\mathrm{m}^3/\mathrm{h}\right]$; and $A_E$ is the envelope area $\left[\mathrm{m}^2\right]$.

### 3.2.3 Infrared thermography

IRT images consist of a series of plain thermal data. This data is analyzed using IRT processing software, which interpolates temperature values captured by the camera. For this purpose, the obtention of materials' parameters, especially IR emissivity ($\varepsilon$), is needed. IR emissivity is the property that materials have for emitting thermal radiant energy to the media. This depends on multiple characteristics of the material such as density, texture, and composition, among others, but not color or lighting.

Perfect emissivity ($\varepsilon = 1$) is only theoretically defined by the "black body." Other materials have an emissivity value below 1. To set up the emissivity in the IRT camera, black thermal insulation tape is used. This tape glued to the surface under study acquires the temperature of that surface in a couple of minutes. The emissivity is set by screening the temperature registered on the tape. Also, the picture can be adjusted using the image treatment software.

Thermal radiant energy comes from everywhere in space, so it is necessary to discard the energy reflected by the analyzed surface, other objects, or people. The most common process to do so is configuring the ambient temperature in the thermal IR imaging camera and discarding the thermal radiant energy reflected in the space. This is possible using Lambert's radiator, which provides the value of the emissivity part of the energy captured by the IR sensor within the camera. Lambert's radiator creates a diffuse reflection whose radiant temperature is a mix of the radiant temperatures coming from all the surfaces in the space. To set the ambient temperature of the reflected thermal radiation, the radiant temperature of Lambert's radiator is measured, adjusting its emissivity as a perfect black body ($\varepsilon = 1$). This is commonly known as radiant temperature correlation (RTC).

Every IRT equipment captures the IR thermal radiation emitted by the surface under study, the reflection of the IR thermal radiant energy of the ambient and the transmission of the IR thermal radiant energy along the object or surface, which is usually negligible.

This non-destructive evaluation is normally used to evaluate energy losses, for detecting a lack of insulation in the envelope of conditioned spaces (Fox et al., 2014), but also to locate moisture in building components and as a diagnosis tool of the building envelope (Barreira et al., 2016). A more advanced method is the detection of leakages through the envelope (Kirimtat & Krejcar, 2018). This is possible since air infiltration through building elements involves temperature differences on its surfaces that can be measured by IRT. The application of IRT to assess the airtightness and thermal insulation of the building envelope was thoroughly detailed by Pettersson and Axen (1980).

Leakages allow the air in and out through the building envelope. If the space is normally conditioned, it impacts the global energy efficiency of the building. Using IRT, air leakages can be located by analyzing the temperature difference between the air leakage affection area and a reference temperature in a close surface. The reference temperature is commonly obtained from the close nonaffected surface.

However, IRT also involves some limitations. It is demonstrated that sometimes the air is exchanged through different paths, such as building systems, crawl spaces, or ducts. In multiple-layer walls, the air may enter the air chamber between fabric or plaster layers from cracks in the external layer and get inside through leaks in the inner layer. This promotes a phenomenon of indirect air infiltration, which is not suitable for its full evaluation using IRT because of the preheating process in the air chamber (Janssens, 2003). In this case, alternative evaluation processes are needed.

Although IRT is usually applied to locate leakages, some authors have also developed a method for the quantitative assessment of air leaks: to evaluate the

contribution of airtightness of building components (Barreira et al., 2017), to take an approximation to the surface area of the gap (Dufour et al., 2009), and to calculate the airflow through the gap (Baker et al., 1987), which all together define the air infiltration rate in buildings (Liu et al., 2018). This kind of analysis requires the evaluation of the characteristics of the building materials in the affection area, specially referred to as energy heat transfer. Its use in the detection of pathologies in historical and heritage buildings is useful (Tavukçuoğlu et al., 2018). This knowledge can give technicians a great amount of information for the evaluation of retrofitting strategies.

### 3.2.4 Infrared thermography combined with pressurization

The use of combined IRT and pressurization of the building envelope has become a common practice (Eskola et al., 2015; Feijó-Muñoz et al., 2018; Gillott et al., 2016; Tanyer et al., 2018). Pressurization tests are used to quantify the airtightness but no information regarding leakage location is given. This combined method allows for the identification of leakages provided that there is enough temperature difference between the indoor and outdoor environments (ISO 9972,72, 2015).

Outdoor air enters the room forced by the depressurization created by the fan through the leaks, causing a quick temperature difference in the surface surrounding the gap of the envelope of the conditioned space. In this sense, it is important to avoid confusing leakage paths and thermal bridges, which often are concentrated around the same areas (Charlesworth, 1988). To avoid it, image subtraction or image comparison between natural and pressurized conditions is often performed (Kalamees, 2007; Vollmer & Möllmann, 2017). In such cases, the reference temperature used is that registered before the air exchange, identifying the air leakage impact by comparing temperature data along the time (Fox et al., 2015).

The first step in the study is to prepare the space to take good-quality IR thermal images. A good way is to cover all the lamps and bulbs which use incandescent technologies with rugs, clothes, or rigid panels because they emit thermal IR radiation (longwave radiation). This can badly affect the identification of air leakages using IR thermal imaging.

After that, several IRT images are taken inside, focusing especially on the usual leakage paths (Fig. 3.11). A Flir e75 IR thermal camera is used to picture leakages. These are typically found in joints such as window frames, materials joints, wall cracks, electrical and sanitary grids, wall-mounted and ceiling lighting and other security facilities such as smoke detectors or emergency lighting in ceilings, and so on. The IR thermal camera has a $320 \times 240$ (76,800 pixels) resolution with an object temperature range of $-20°C$ to $120°C$ in an 18 mm lens.

For that, it is necessary to identify each material's emissivity. A black thermal insulation tape is positioned close to the area to be IR thermally captured. After 5 minutes, the surface of the tape acquires the temperature of the surface object of the IR thermal picture. The IRT camera can be set up by adjusting the emissivity as previously defined or evaluated with software. These IR thermal images are used as reference temperature indicators in the assumed areas of affection of the air leakages.


**Figure 3.11 Typical leakage paths.** (A) Window frames, (B) material joints, (C) wall cracks, (D) electrical grids, (E) ceiling holes for facilities, and (F) plafonds.

The emissivity values reached for the different construction materials in the room are shown in Table 3.2.

Before turning on the blowing fan, further thermal data must be registered by a term hygrometer. The outdoor temperature (2.8°C) is lesser than indoors (22.4°C), with a thermal difference of 19.6°C. Humidity is constant inside and outside. RTC is adjusted by placing the Lamberts' radiator close to the surface to be photographed. RTC value is the same (22.4°C) so no adjustment is needed.

Next, the blowing fan is set up in the position of depressurization, forcing the air coming from outdoors to enter the space through the leakage paths of the envelope. Depressurization is set up to a 50 Pa pressure difference (between inside and outside)

**Table 3.2** Materials'emissivity in the room.

| Position | Surface material | Emissivity ($\varepsilon$) |
|---|---|---|
| Ceiling | Painted plain plaster | 0.90 |
| Walls | Painted rough plaster | 0.89 |
| Walls (skirting board) | Vanished plain wood | 0.87 |
| Walls (bathroom) | Polished tiles | 0.92 |
| Windows | Painted plain wood | 0.94 |
| Windows | Glass | 0.95 |
| Windows | Painted metal | 0.97 |
| Floor | Vanished specular wood | 0.89 |

in "cruise configuration." This pressure difference guarantees a quick transfer of thermal energy by the air entering the space and the air leakage affection areas. In winter conditions, the incoming air makes the temperature of the envelope surface decrease from that registered as a reference. After 5−10 minutes, the thermal IR images are taken. The surface differential temperature will focus the attention on the defying infiltration gap.

After the images are taken, every image is processed using specialized software by adjusting those parameters that are difficult to set during the test.

## 3.3 Results

### *3.3.1 Air permeability*

The pressurization test to measure the air permeability of the guesthouse room was carried out between 10:00 a.m. and 12:00 p.m. The average outdoor temperature was 2°C with 75% relative humidity. The wind speed was on average 1.39 m/s from the northwest. Therefore environmental conditions were favorable and within the limits stated in ISO 9972. Indoor/outdoor temperature difference, expressed in Kelvin, multiplied by the height, expressed in meters, was lesser than 250 mK. Regarding wind speed, the limits were not reached and kept always below 3 on the Beaufort scale.

Initially, the test was performed considering the whole volume of the room (Test 1). Extremely high permeability results and the hypothesis that most of the airflow could come from the bathroom motivated the performance of a second pressurization test excluding its volume (Test 2). The configuration of both tests is shown in Fig. 3.12.

Table 3.3 and Fig. 3.13 show the results obtained regarding the airtightness of the envelope.

The obtained coefficient of determination $r^2$ was greater than 0.98, thus the tests can be considered valid.

The air change rate at 50 Pa obtained in Test 1 is extremely high. Results improve significantly when excluding the bathroom volume (Test 2), so it can be

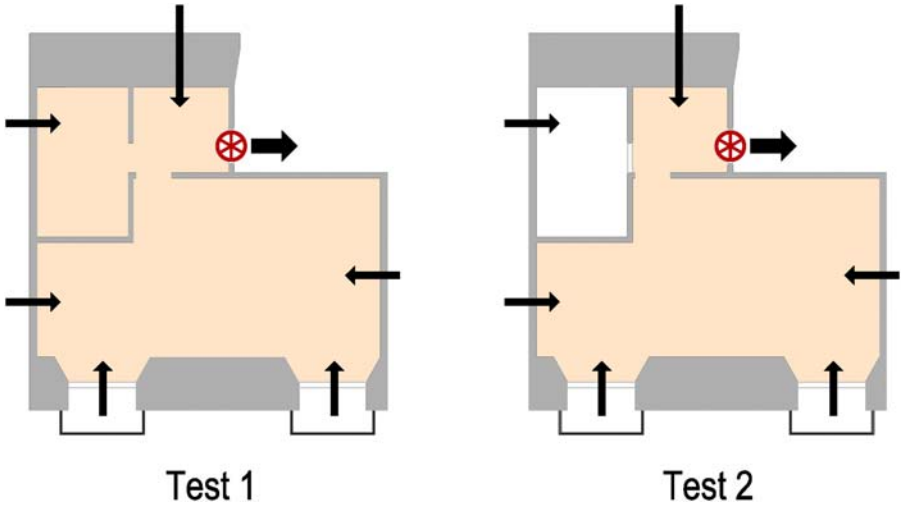


**Figure 3.12 Airtightness test configuration.** Test 1 (whole room) and Test 2 (excluding the bathroom).

stated that important leakages are located in this area. Although results are not comparable due to the different typologies and construction technologies, the airtightness of the room is close to the average $n_{50}$ values reported for multifamily buildings in this area (Feijó-Muñoz et al., 2019).

The coefficient $n$ values obtained close to 0.5 are a symptom of the leaky envelope. It must be noted that especially for Test 1, the airflow is almost fully turbulent, and it is clear the presence of large leakage paths. Regarding Test 2, a slight improvement can be observed, by adding a laminar component. Nevertheless, the values obtained for Test 2 are in agreement with other test results reported in this area (Feijó-Muñoz et al., 2019).

Finally, it can be observed in the graphs that the airflow rates during the pressurization stage are larger in both cases than the ones during depressurization. This can be explained by the fact that the building is subject to unnatural conditions, which can alter the leakage characteristics, especially false ceilings, traps, or some kinds of windows (Charlesworth, 1988). Leakage curves do not overlap as a result of a possible valving effect or asymmetric geometry of some leakages in relation to the flow direction (Allen, 1985; Baker et al., 1986).

### 3.3.2 Evaluation of leakages

The analysis of the permeability values shows the lack of airtightness of the envelope. However, the blower door test did not provide information regarding leakage location and characterization. IRT is then useful for its location and identification.

Fig. 3.14 shows a comparison of the IR thermal images taken before and after depressurization. The air leakage affection area is in this way shown. All the

**Table 3.3** Pressurization tests results.

| | **Depressurization** | | | | | **Pressurization** | | | | | **Average values** | | |
|---|---|---|---|---|---|---|---|---|---|---|---|---|---|
| | [$m^3$/h] | $n_{50}$[$h^{-1}$] | $q_{50}$[$m^3$/$m^2$h] | [-] | $r^2$ [-] | $Q_{50}$[$m^3$/h] | $n_{50}$[$h^{-1}$] | $q_{50}$[$m^3$/$m^2$h] | [-] | $r^2$ [-] | $Q_{50}$[$m^3$/h] | $n_{50}$[$h^{-1}$] | $q_{50}$[$m^3$/$m^2$h] |
| Test 1 | 5296 | 51.53 | 36.86 | 0.51 | 0.996 | 6859 | 66.74 | 47.74 | 0.57 | 0.989 | 6078 | 59.14 | 42.30 |
| Test 2 | 628 | 7.33 | 4.67 | 0.61 | 0.999 | 692 | 8.07 | 5.14 | 0.61 | 0.995 | 660 | 7.70 | 4.90 |

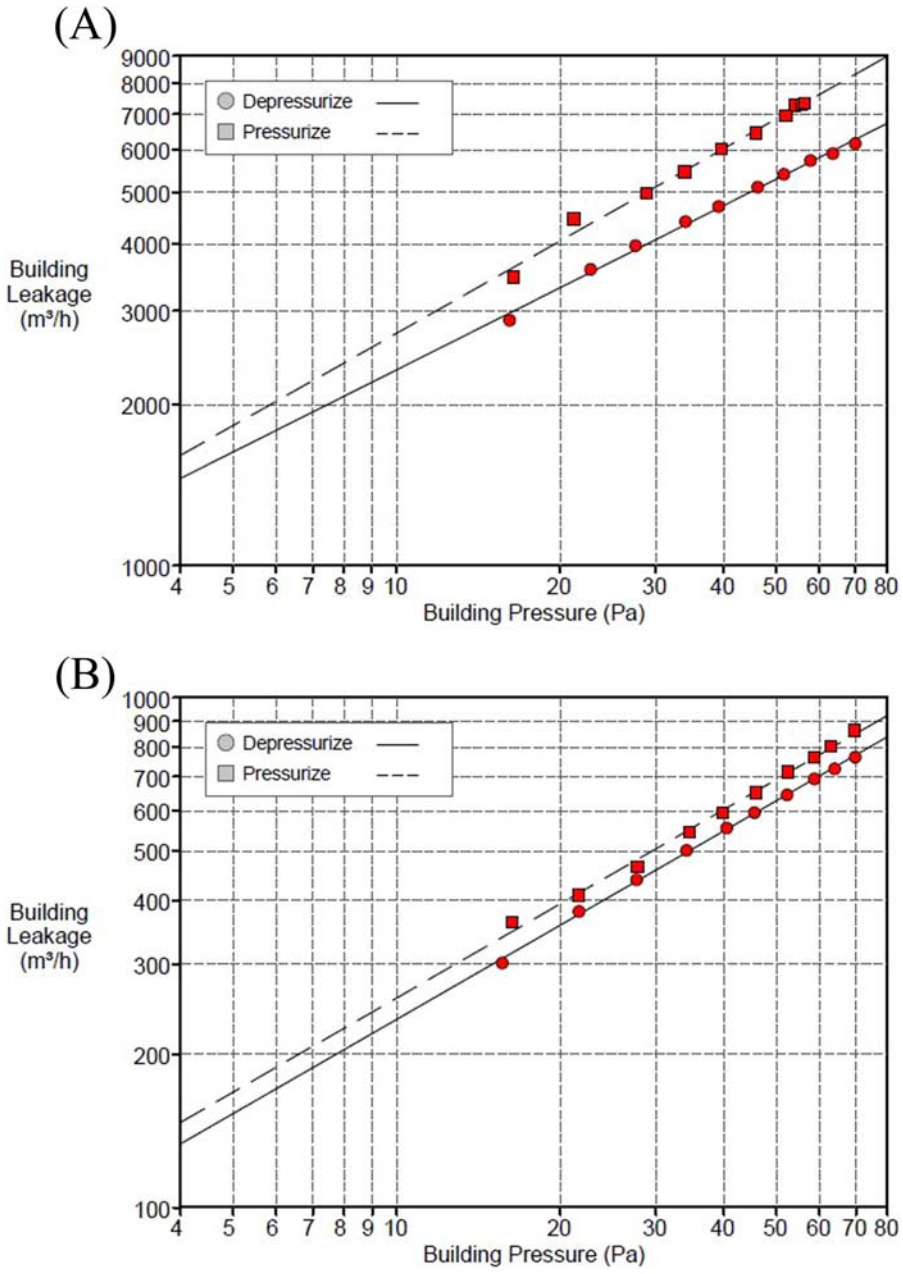


**Figure 3.13 Pressurization tests graphs.** (A) Test 1 graph (whole volume of the room) and (B) Test 2 graph (volume of the room excluding the bathroom).

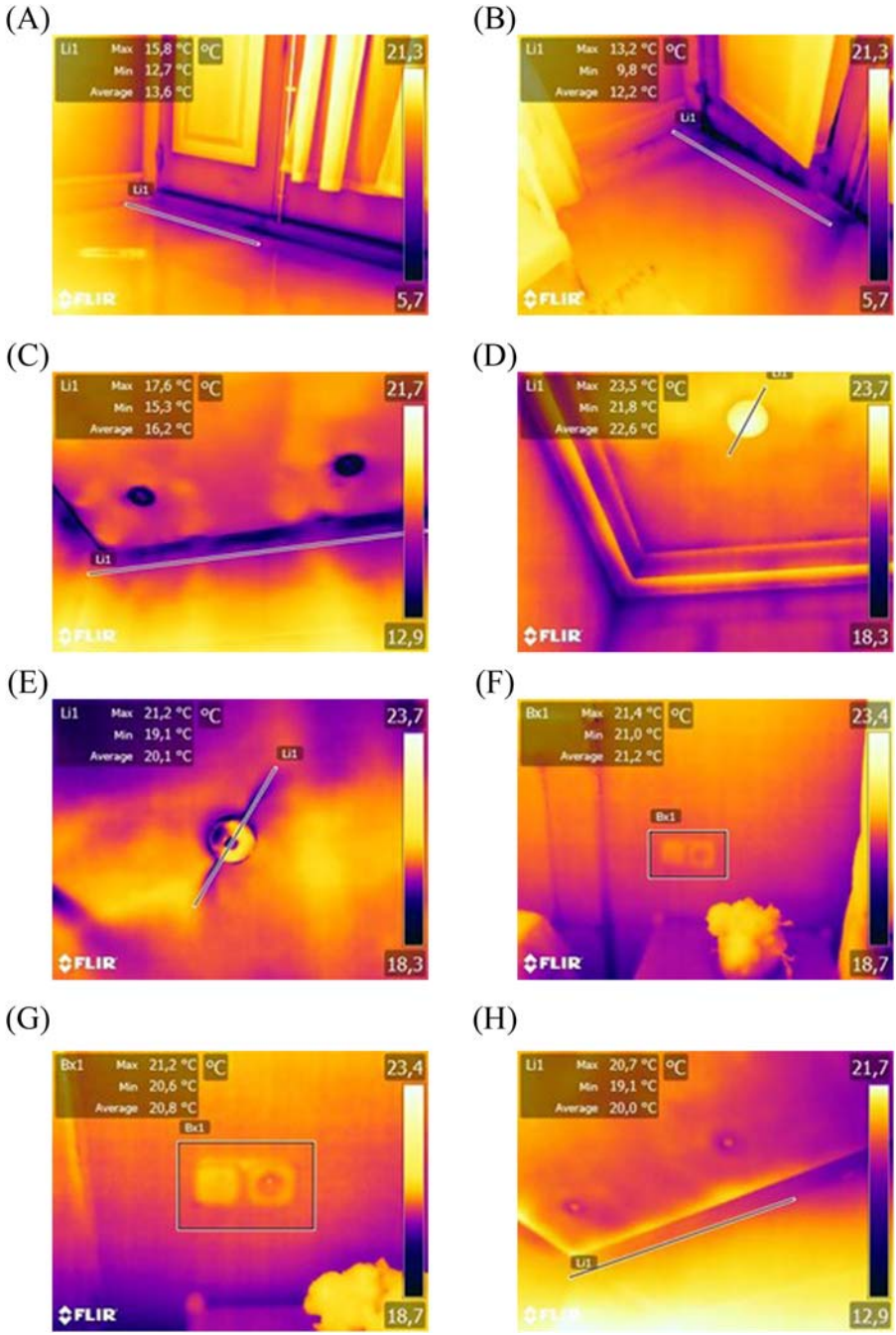


**Figure 3.14 Comparison of the IR thermal images taken before and after depressurization.** (A) Representative wooden door-window before depressurization test (floor emissivity ε = 0.89), (B) Representative wooden door-window after depressurization test (floor emissivity ε = 0.89), (C) Materials joints in bathroom before depressurization test (wall tiles emissivity ε = 0.92), (D) Materials joints in bathroom after depressurization test (wall tiles emissivity ε = 0.92), (E) Ceiling holes for smoke detector before depressurization test (ceiling emissivity ε = 0,90), (F) Ceiling holes for smoke detector after depressurization test (ceiling emissivity ε = 0,90), (G) Electrical grids before depressurization test (wall plaster emissivity ε = 0,89), (H) Electrical grids after depressurization test (wall plaster emissivity ε = 0,89). *IR*, Infrared.

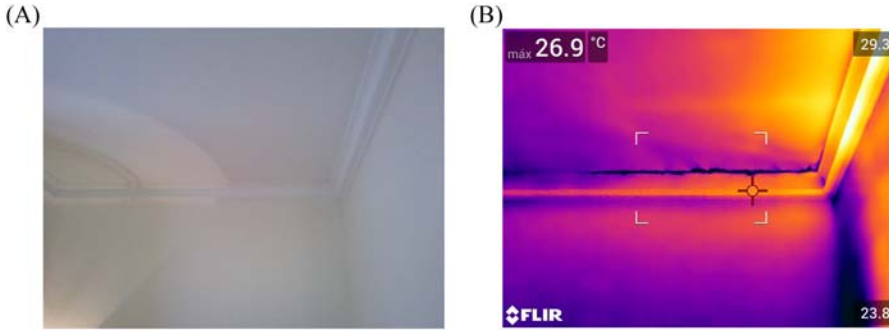


**Figure 3.15 Corner cracks.** (A) Picture and (B) IR thermal image. *IR*, Infrared.

coupled IR thermal images were adjusted to the same temperature range and a reference temperature line is defined for their comparison.

From these results, it can be assumed that window frames made of wood were not airtight, letting infiltrating air pass through their joints even at natural building pressure difference. Wall-mounted electrical grids did not involve any important air leakage. However, most of the air infiltration has its origin in the ceiling. It is assumed that there is a highly ventilated crawl space above the room between the room and the roof made of tiles. This was presumed from the observation of three different facts: (1) most of the air enters through the bathroom ceiling perimeter, which lacks joints to the walls; (2) the air infiltration affection area temperature decayed close to the holes made on the ceiling; and (3) corner cracks between ceiling and walls were identified (Fig. 3.15).

## 3.4 Discussion

The application of pressurization tests combined with IRT allowed both the quantification of the airtightness of the room envelope and the location of the main leakages.

Results show that the room is extremely leaky when including the bathroom volume. The evaluation of the envelope led to the hypothesis that the false ceiling is somehow connected to the crawl space above, letting unconditioned air enter the room, especially through the bathroom. This is supported by the results obtained in Test 2, but also IR thermal images show clear leakages in every discontinuity of the false ceiling: lights, smoke detector, or cracks. To prove this assumption, the ventilated roof crawl space was accessed, and the construction configuration was evaluated.

The hypothesis of a nonfinished false ceiling and insulation was then proved. As can be observed in Fig. 3.16, the wooden platform of the ceiling and the insulation show important discontinuities and even holes of great dimensions. Furthermore, the ventilation exhaust of the bathroom is open and not connected to the exhaust duct. This clearly explains the airtightness test results, which constituted a key element in the diagnosis of the energy performance of the room.


**Figure 3.16 Upper crawl space.** (A) General view and (B) detail of the construction elements.

The perimeter of windows also concentrates important leakage paths, especially in the joint with the pavement. In contrast, electrical grids and other discontinuities in the walls did not involve important temperature difference. This can be explained due to the masonry construction system of the dividing walls. This construction practice is now uncommon since new buildings usually integrate light plaster walls, which promote air exchange through the inner air chamber. When this chamber connects different spaces or even the outdoor air, the air can be freely exchanged through electrical grids, pipes, or any other open device.

## 3.5 Conclusion

The evaluation of the envelope of historic buildings requires the application of NDT, which does not alter its characteristics. In the case of energy audits and energy retrofitting solutions, a good diagnosis is key in the decision-making process. In this sense, the airtightness of the envelope is the main characteristic that involves air infiltration. Uncontrolled airflows across the building envelope led to a phenomenon that involves air mass exchange between the indoors and outdoors, and, thus, energy transfer and unnecessary energy use.

This chapter presents a methodology based on the combination of pressurization tests and IRT to quantify the airtightness of the envelope and to locate the main leakages. The method was then applied to a room in the Hospedería del Colegio Santa Cruz. Although in plain sight no pathologies were found and no inadequate performance had been reported, the assessment of the envelope airtightness showed hidden construction issues which seriously compromise the energy performance of the building.

The study demonstrated that air infiltration detected using IRT technology is due to several circumstances. Leaks were identified around the window frames. This can be related to material compatibility. The wood in the window frames can change its dimensions along its life, and, when no elastic joints are included, discontinuities and cracks allow the air to infiltrate.

On the other hand, the main leakages are related to the lack of airtightness and insulation of the room ceiling and the roof crawl space above, especially in the bathroom area. The inclusion of a light plaster false ceiling hides this and makes it almost impossible to identify this construction problem. This false ceiling contains multiple holes and leakages around several devices (speakers), lighting or security (smoke sensors or emergency lighting), and also some cracks near one of the corners of the room. This was further evaluated by observation from the crawl space. Clear gaps and unfinished construction elements explained the lack of airtightness. That creates a path for air transfer between spaces with different thermal conditions, which impacts the surface temperature close to those leakages. Therefore solving this construction problem constitutes a priority when implementing energy measures and retrofitting actions in the building.

The application of IRT while depressurizing the volume under study was found to be a useful method to identify weak points of the envelope without degrading the construction. This NDT proved to be crucial to evaluate the performance of the building envelope before proposing energy retrofitting solutions.

## References

Allen, C. (1985). *Technical Note AIC 16. Leakage distribution in buildings*.

ASHRAE. (2021). *ASHRAE Handbook - Fundamentals*.

Baker, P. H., Sharples, S., & Ward, I. C. (1987). Air flow through cracks. *Building and Environment*, *22*(4), 293−304. Available from https://doi.org/10.1016/0360-1323(87)90022-9.

Baker, P. H., Sharples, S., & Ward, I. C. (1986). Air flow through asymmetric building cracks. *Building Services Engineering Research & Technology*, *7*(3), 107−108. Available from https://doi.org/10.1177/014362448600700302.

Barreira, E., Almeida, R. M. S. F., & Delgado, J. M. P. Q. (2016). Infrared thermography for assessing moisture related phenomena in building components. *Construction and Building Materials*, *110*, 251−269. Available from https://doi.org/10.1016/j.conbuildmat.2016.02.026.

Barreira, E., Almeida, R. M. S. F., & Moreira, M. (2017). An infrared thermography passive approach to assess the effect of leakage points in buildings. *Energy and Buildings*, *140*, 224−235. Available from https://doi.org/10.1016/j.enbuild.2017.02.009.

Bohac, D., Schoenbauer, B., Fitzgerald, J. (2016). Using an aerosol sealant to reduce multifamily envelope leakage. *ACEEE Summer Study on Energy Efficiency in Buildings*, pp. 1−16.

Charlesworth, P.S. (1988). *Air exchange rate and airtightness measurement techniques - An applications guide*. Air Infiltration and Ventilation Centre.

Directive 2018/844 amending Directive 2010/31/EU on the energy performance of buildings and Directive 2012/27/EU on energy efficiency. 156 (2018).

Domínguez-Amarillo, S., Fernández-Agüera, J., Campano, M. Á., & Acosta, I. (2019). Effect of airtightness on thermal loads in legacy low-income housing. *Energies*, *12*(9). Available from https://doi.org/10.3390/en12091677, https://www.mdpi.com/1996-1073/12/9.

Dufour, M. B., Derome, D., & Zmeureanu, R. (2009). Analysis of thermograms for the estimation of dimensions of cracks in building envelope. *Infrared Physics and Technology*, *52*(2−3), 70−78. Available from https://doi.org/10.1016/j.infrared.2009.01.004.

Eskola, L., Alev, Û., Arumägi, E., Jokisalo, J., Donarelli, A., Sirén, K., & Kalamees, T. (2015). Airtightness, air exchange and energy performance in historic residential buildings with different structures. *International Journal of Ventilation*, *14*(1), 11−26. Available from https://doi.org/10.1080/14733315.2015.11684066, http://ijovent.org/doi/pdf/10.5555/2044-4044-14.1.11.

Feijó-Muñoz, J., González-Lezcano, R. A., Poza-Casado, I., Padilla-Marcos, M. Á., & Meiss, A. (2019). Airtightness of residential buildings in the Continental area of Spain. *Building and Environment*, *148*, 299−308. Available from https://doi.org/10.1016/j.buildenv.2018.11.010, http://www.elsevier.com/inca/publications/store/2/9/6/index.htt.

Feijó-Muñoz, J., Poza-Casado, I., González-Lezcano, R. A., Pardal, C., Echarri, V., De Larriva, R. A., Fernández-Agüera, J., Dios-Viéitez, M. J., Campo-Díaz, V. J. D., Calderín, M. M., Padilla-Marcos, M. Á., & Meiss, A. (2018). Methodology for the study of the envelope airtightness of residential buildings in Spain: A case study. *Energies*, *11* (4), 704. Available from https://doi.org/10.3390/en11040704.

Fernández, Cantera, García. (2010). Universidad de, Valladolid, Locus sapientiae: la Universidad de Valladolid en sus edificios. Consejo Social,.

Filippidou, F., Navarro, J.P. (2019). *Achieving the cost-effective energy transformation of Europe's buildings*. Publications Office of the European Union. 29906, Available from https://doi.org/10.2760/278207.

Fox, M., Coley, D., Goodhew, S., & De Wilde, P. (2015). Time-lapse thermography for building defect detection. *Energy and Buildings*, *92*, 95−106. Available from https://doi.org/10.1016/j.enbuild.2015.01.021, https://www.journals.elsevier.com/energy-and-buildings.

Fox, M., Coley, D., Goodhew, S., & De Wilde, P. (2014). Thermography methodologies for detecting energy related building defects. *Renewable and Sustainable Energy Reviews*, *40*, 296−310. Available from https://doi.org/10.1016/j.rser.2014.07.188.

Gillott, M. C., Loveday, D. L., White, J., Wood, C. J., Chmutina, K., & Vadodaria, K. (2016). Improving the airtightness in an existing UK dwelling: The challenges, the measures and their effectiveness. *Building and Environment*, *95*, 227−239. Available from https://doi.org/10.1016/j.buildenv.2015.08.017, http://www.elsevier.com/inca/publications/store/2/9/6/index.htt.

Huang, J., Hanford, J., Yang, F. (1999). *Residential heating and cooling loads component analysis*.

ISO 9972. (2015). *Thermal performance of buildings. Determination of air permeability of buildings. Fan pressurization method*. 9972.

Janssens, A. (2003). Methodology for measuring infiltration heat recovery for concentrated air leakage. In Research in Building Physics: *Proceedings of the Second International Conference on Building Physics* (pp. 14−18), CRC Press.

Jokisalo, J., Kurnitski, J., Korpi, M., Kalamees, T., & Vinha, J. (2009). Building leakage, infiltration, and energy performance analyses for Finnish detached houses. *Building and Environment*, *44*(2), 377−387. Available from https://doi.org/10.1016/j.buildenv.2008.03.014.

Jones, B., Das, P., Chalabi, Z., Davies, M., Hamilton, I., Lowe, R., Mavrogianni, A., Robinson, D., & Taylor, J. (2015). Assessing uncertainty in housing stock infiltration rates andassociated heat loss: English and UK case studies. *Building and Environment*, *92*, 644−656. Available from https://doi.org/10.1016/j.buildenv.2015.05.033, http://www.elsevier.com/inca/publications/store/2/9/6/index.htt.

Kalamees, T. (2007). Air tightness and air leakages of new lightweight single-family detached houses in Estonia. *Building and Environment*, *42*(6), 2369−2377. Available from https://doi.org/10.1016/j.buildenv.2006.06.001.

Kirimtat, A., & Krejcar, O. (2018). A review of infrared thermography for the investigation of building envelopes: Advances and prospects. *Energy and Buildings*, *176*, 390−406. Available from https://doi.org/10.1016/j.enbuild.2018.07.052.

Kronvall, J. (1980). *Airtightness measurements and measurement methods*. Swedish Council for Building Research, Stockholm, Sweden. https://www.aivc.org/resource/airtightness-measurement-and-measurement-methods-matningar-och-matmetoder-lufttathet.

Lerma, C., Mas, Á., Gil, E., Vercher, J., & Peñalver, M. J. (2014). Pathology of building materials in historic buildings. Relationship between laboratory testing and infrared thermography. *Materiales de Construcción*, *64*(313), e009. Available from https://doi.org/10.3989/mc.2013.06612.

Liu, W., Zhao, X., & Chen, Q. (2018). A novel method for measuring air infiltration rate in buildings. *Energy and Buildings*, *168*, 309−318. Available from https://doi.org/10.1016/j.enbuild.2018.03.035, https://www.journals.elsevier.com/energy-and-buildings.

Lucchi, E. (2018). Applications of the infrared thermography in the energy audit of buildings: A review. *Renewable and Sustainable Energy Reviews*, *82*, 3077−3090. Available from https://doi.org/10.1016/j.rser.2017.10.031, https://www.journals.elsevier.com/renewable-and-sustainable-energy-reviews.

McWilliams, J. (2003). *AIVC Annotated Bibliography 12. Review of air flow measurement techniques*. Air Infiltration and Ventilation Centre.

Meiss, A., & Feijó-Muñoz, J. (2015). The energy impact of infiltration: a study on buildings located in north central Spain. *Energy Efficiency*, *8*(1), 51−64. Available from https://doi.org/10.1007/s12053-014-9270-x, http://www.springer.com/environment/journal/12053.

Ordax, A. (2005). Santa Cruz, arte e iconografía: el Cardenal Mendoza, El Colegio y los colegiales. *Ediciones Institucionales*, *124*.

Pettersson, B., Axen, B., (1980). *Thermography: Testing of the thermal insulation and air-tightness of buildings*. Swedish Council for Building Research, Stockholm.

Pickering, P. L., Cucchiara, A. L., Gonzales, M., & McAtee, J. L. (1987). Test ventilation with smoke, bubbles, and balloons. *ASHRAE Transactions*, *2*.

Priestner, R., Steel, A.C., (1991). *Air flow patterns within buildings measurement techniques*. Technical Note AIVC. Air Infiltration and Ventilation Centre, Coventry, Great Britain, https://www.aivc.org/resource/tn-34-air-flow-patterns-within-buildings-measurement-techniques.

Sherman, M.H., & Chan, R., (2004). *Building airtightness: Research and practice*.

Simson, R., Rebane, T., Kiil, M., Thalfeldt, M., Kurnitski, J. (2020). The impact of infiltration on heating systems dimensioning in Estonian climate. *E3S Web of Conferences*. 10.1051/e3sconf/202017205004 22671242 EDP Sciences Estonia. http://www.e3s-conferences.org/ 172.

Tanyer, A. M., Tavukcuoglu, A., & Bekboliev, M. (2018). Assessing the airtightness performance of container houses in relation to its effect on energy efficiency. *Building and Environment*, *134*, 59−73. Available from https://doi.org/10.1016/j.buildenv.2018.02.026, http://www.elsevier.com/inca/publications/store/2/9/6/index.htt.

Tavukçuoğlu, A., Diouri, A., Boukhari, A., Ait Brahim, L., Bahi, L., Khachani, N., Saadi, M., Aride, J., & Nounah, A. (2018). Non-destructive testing for building diagnostics and

monitoring: Experience Achieved with case studies. *MATEC Web of Conferences*, *149*, 01015. Available from https://doi.org/10.1051/matecconf/201814901015.

Vollmer, Michael, & Möllmann, Klaus-Peter (2017). *Fundamentals of infrared thermal imaging* (pp. 1−106). Wiley. Available from 10.1002/9783527693306.ch1.

Zheng, Xiaofeng, Cooper, Edward, Gillott, Mark, & Wood, Christopher (2020). A practical review of alternatives to the steady pressurisation method for determining building airtightness. *Renewable and Sustainable Energy Reviews*, *132*110049. Available from https://doi.org/10.1016/j.rser.2020.110049.

WOODHEAD PUBLISHING SERIES IN CIVIL AND STRUCTURAL ENGINEERING

Heritage buildings crucially contribute to the economy of those countries that rely heavily on the tourism industry. Investigation and monitoring of the origins of deterioration and damage are therefore key to the preservation of historical and cultural assets. ***Diagnosis of Heritage Buildings by Non-destructive Techniques*** offers an up-to-date overview of the latest knowledge by compiling specialized studies written by an international group of experts in the field. The volume is an invaluable reference resource for students, researchers, and practitioners alike.

## Key Features

- Helps readers easily identify the latest advances in non-destructive testing by subdividing the content into sections specific to each assessment approach
- Explores the integration of different NDT methodologies, facilitating the interoperability of traditional and advanced technologies
- Presents case studies based on real built heritage to show how to correctly implement the measurement techniques described and to interpret the results

## About the Editors

**Blanca Tejedor Herrán** works as an Associate Professor at the Department of Project and Construction Engineering of the Polytechnic University of Catalonia since 2021. Her research expertise is focused on the implementation of quantitative infrared thermography for building diagnosis, the assessment of indoor thermal comfort, and the smart management of building facilities. In recent years, she has collaborated with more than 12 universities and research centers at national and international levels. Currently, Dr. Tejedor is an officer of the Data Sensing and Analysis (DSA) Committee of the European Council on Computing in Construction (EC3).

**David Bienvenido-Huertas** is an Assistant Professor at the Department of Building Construction of the University of Granada. He is also a Visiting Professor at the University of La Coruña. His area of expertise covers climate change in the building sector, adaptive thermal comfort, heat transfer, fuel poverty, energy conservation measures, and design of nearly zero-energy buildings. He has been included in the World's Top 2% Scientists List made by Stanford University and ELSEVIER (2020 and 2021).

ELSEVIER
WP
WOODHEAD PUBLISHING
An imprint of Elsevier
elsevier.com/books-and-journals

ISBN 978-0-443-16001-1
9 780443 160011